

# Properties of hadrons in lattice quantum chromodynamics with dynamical Wilson fermions

Herbert W. Hamber

*Department of Physics, University of California at Irvine, Irvine, California 92717*

(Received 31 May 1988)

New results of a large-scale simulation of lattice quantum chromodynamics with three ( $u, d, s$ ) dynamical Wilson fermions on a  $10 \times 10 \times 10 \times 30$  space-time lattice are presented. The computations presented here confirm earlier results that indicated the presence of substantial effects due to fermion vacuum-polarization loops. As a check on the results two values for the gauge coupling constant are considered and some degree of scaling is observed. The quark mass dependence of the physical pseudoscalar-meson mass is explicitly determined both in the case of equal-mass and unequal- (heavy-light) mass systems, as well as in the case of light sea quarks versus heavy valence quarks, with the latter situation being relevant for heavy-quark bound states. Further results include estimates for other lowest-lying hadron masses, for the (current-algebra) quark masses ( $m_u, m_d, m_s$ , and  $m_c$ ), and for the pseudoscalar-meson decay constants ( $f_\pi, f_K, f_D, f_{\eta_c}$ , and  $f_B$ ). An estimate of the strangeness content of the proton is given. Relatively small mass values are found for the light quarks ( $u, d, s$ ). In the case of the decay constants the full lattice QCD estimates could give new predictions, since some of the experimental values are not known yet.

## I. INTRODUCTION

Considerable progress has recently been made in understanding nonperturbative effects in QCD using numerical methods for the lattice formulation. Of great interest in QCD is the hadron spectrum and the hadron's wave functions, since a wealth of experimental data has been available for quite some time. Some decay constants which can be computed with relative ease in lattice QCD ( $f_D, f_B, \dots$ ) will soon be measured in accelerator experiments<sup>1,2</sup> and thus provide a relatively stringent test for the predictive power of (lattice) QCD. The values of the quark masses<sup>3</sup> are also of substantial importance, since they can impose constraints on the grand unified model and provide a view on the properties of the ultimate constituents of matter. Because of quark confinement these masses can only be inferred indirectly from the observed hadron states. Needless to say, a precise knowledge of the quark masses is an essential ingredient in models that attempt to predict the properties of yet-unobserved quarks (such as the top quark) by resorting to simple physical models of level mixing.<sup>4</sup>

Since most of the lattice QCD computations have been done neglecting fermion vacuum-polarization contributions (see, for example, Ref. 5 and references therein, and for reviews see Refs. 6 and 7), one of the outstanding problems that has remained is the development of a set of efficient algorithms to reliably include these effects in a realistic study of the full low-energy spectrum of QCD. In this work results will be presented (some of which have already appeared in the second of Ref. 8) which extend previous computations done by the author on smaller lattices (first of Ref. 8). Furthermore, only the Wilson fermions ( $r=1$ ) will be considered in the following. It appears at the present moment that the pseudofermion method<sup>9</sup> is among the more promising methods for including the effects of dynamical fermions and it is the purpose of this paper to describe results obtained on a

relatively large lattice when the effects of the fermion loops are included this way.

## II. GENERAL METHODOLOGY

Only a rather brief summary of the methods will be presented here, since adequate and more detailed expositions already exist in the literature. The purpose of this section is mainly to establish notation and comment on possible sources of errors, to which later sections will refer. The total lattice QCD action<sup>10</sup> consists of a gauge contribution

$$S_G = -\frac{\beta}{6} \sum_{n, \mu < \nu} \text{Tr} U_{n, \mu} U_{n+\mu, \nu} U_{n+\nu, \mu}^\dagger U_{n, \nu}^\dagger + \text{c.c.} \quad (1)$$

and a fermion contribution

$$S_F = k \sum_f \sum_{n, \mu} [\bar{\psi}_n^{(f)} (1 + \gamma_\mu) U_{n\mu} \psi_{n+\mu}^{(f)} + \bar{\psi}_{n+\mu}^{(f)} (1 - \gamma_\mu) U_{n\mu}^\dagger \psi_n^{(f)}] - \sum_f \sum_n \bar{\psi}_n^{(f)} \psi_n^{(f)}, \quad (2)$$

where the  $U$ 's are  $3 \times 3$  complex matrix elements of the group  $SU(3)$  and the  $\gamma$ 's are Euclidean gamma matrices ( $\{\gamma_\mu, \gamma_\nu\} = 2\delta_{\mu\nu}, \gamma_\mu^\dagger = \gamma_\mu$ ). The gauge coupling  $g$  is as usual related to  $\beta$  by  $\beta = 6/g^2$ , for simplicity the lattice spacing  $a$  is set equal to one in most of the following, and the lattice is taken to be periodic of size  $L \times L \times L \times T$ . In this paper  $L = 10$  and  $T = 30$ , and  $\beta = 5.3$  and  $\beta = 5.4$ . The number of fermion flavors  $n_f$  will be taken to be 3, a choice which appears reasonable if one wants to investigate the properties of light hadrons composed of  $u, d$ , and  $s$  quarks. For simplicity in the following all "sea quark" flavors are assumed to have equal mass.

The fields  $\psi$  and  $\bar{\psi}$  are of fermionic nature and have to be integrated over in order to be able to perform a numerical simulation. In the pseudofermion method the change in the effective action  $\delta S_{\text{eff}}$  (obtained by integrat-

ing out the fermion fields) is first expanded to lowest order in  $\delta U$ , and terms of higher order in  $\delta U$  are neglected.<sup>9</sup> (For more details on the procedure and the errors the reader is referred to the discussions in Refs. 6–9 and 11.) Then one obtains

$$\begin{aligned} \delta S_{\text{eff}} = & \delta S_G - n_f \sum_{n,\mu} [\langle \bar{\psi}_n^a(r + \gamma_\mu) \psi_{n+\mu}^b \rangle \delta U_{n\mu}^{ab} \\ & + \langle \bar{\psi}_{n+\mu}^a(r - \gamma_\mu) \psi_n^b \rangle \delta U_{n\mu}^{ab}] \\ & + O(\delta U^2) \end{aligned} \quad (3)$$

and the angular brackets ( $\langle \rangle$ ) here denote averaging over the fermion fields only, which is achieved by introducing auxiliary scalar (“pseudofermion”) fields. It also replaces the currents in a given gauge field configuration by their averages, which can be computed by a second, separate Monte Carlo process. The procedure introduces an error, the largest contribution being due to the fluctuation in the currents, and which can be estimated to be  $\sim \epsilon n_f^2 / n_{\text{pf}}$  with  $\sqrt{\epsilon}$  parametrizing the smallness of the boson step size  $\delta U$ . The error goes as  $1/n_{\text{pf}}$ , where  $n_{\text{pf}}$  is the number of iterations needed to compute the currents, since the statistical fluctuations in the currents decrease as  $1/\sqrt{n_{\text{pf}}}$  for large samples. In the following  $\epsilon=0.01$  will be considered, and  $n_{\text{pf}}$  will vary between 50 and 100. This choice has proven to be quite adequate for the range of parameters (which include the quark masses and the gauge coupling) explored in this paper, at least as far as the statistical accuracy of the data is concerned. In the future smaller values of  $\epsilon$  will have to be explored to check on the stability of the results, or to perform an extrapolation to vanishing step size.

The masses of the lighter hadrons are obtained by computing the appropriate correlation functions of composite operators and by carefully analyzing their large-distance behavior. In the cases of interest here (meson and baryon states, respectively), they are given by the formulas

$$\begin{aligned} \langle \bar{\psi}\psi(x)\bar{\psi}\psi(0) \rangle_{I \neq 0} &= \int d\mu(U) \text{Tr}[G(x,0|U)G(0,x|U)], \\ \langle \bar{\psi}\bar{\psi}(x)\psi\psi(0) \rangle &= \int d\mu(U) \text{Tr}[G(x,0|U)G(x,0|U)G(x,0|U)], \end{aligned} \quad (4)$$

and color and spinor indices have been suppressed for simplicity. Here  $G(x,0|U) = \langle x | \Delta^{-1}[U] | 0 \rangle$  is the inverse of the lattice Dirac operator  $\Delta[U]$  defined in Eq. (2). The exact full measure  $d\mu[U]$  is given by

$$d\mu(U) = Z^{-1} \prod_{n\mu} dU_{n\mu} \exp(-S_G + n_f \text{Tr} \ln \Delta[U]). \quad (5)$$

The best methods available for computing  $G(x,0|U)$  for large separations rely on an exact numerical iterative inversion of the sparse matrix  $\Delta[U]$ , one column at a time. A necessary condition for convergence is that the matrix  $\Delta[U]$  has no zero eigenvalues, which is satisfied for QCD with massive quarks on a large lattice. In practice no problem was encountered here with the propagator computations since the quark mass was never too small.

Here only meson states are considered which can be created from the vacuum by the local currents  $\bar{\psi}^a(x)\Gamma\psi^a(x)$ , where  $\Gamma$  is a Dirac gamma matrix, and similarly for the baryons. Nonlocal operators provide important information about the wave functions and will be considered in a separate publication. Choices of different operators lead to different propagator amplitudes, but are expected to give the same estimate for the mass of the physical state. It is useful to denote by  $G_M(x)$  and  $G_B(x)$  the generic connected meson and baryon propagators, respectively, averaged over the gauge configurations

$$\begin{aligned} G_M(x) &= \langle \bar{\psi}\psi(x)\bar{\psi}\psi(0) \rangle, \\ G_B(x) &= \langle \bar{\psi}\bar{\psi}(x)\psi\psi(0) \rangle. \end{aligned} \quad (6)$$

From the large-distance behavior of the propagators the hadron masses are then computed by a judicious fit to the appropriate correlation function, summed over spatial hyperplanes to extract the zero spatial momentum state. Since periodic boundary conditions are used, one then expects for the meson propagator the generic behavior

$$\begin{aligned} \tilde{G}_M(t) &\equiv \sum_x G_M(x) \\ &\sim_{t \gg a} 2A_M \cosh \left[ m_M \left[ \frac{T}{2} - t \right] \right] \\ &\quad + 2A_{M^*} \cosh \left[ m_{M^*} \left[ \frac{T}{2} - t \right] \right] + \dots, \end{aligned} \quad (7)$$

where  $m_{M^*}$  is the mass of the first radial recurrence, which can be resolved if  $m_{M^*} - m_M \gg T^{-1}$ , and  $T$  is the temporal extent of the box. On the other hand for the baryons one expects

$$\tilde{G}_B(t) \equiv \sum_x G_B(x) \sim_{t \gg a} \frac{1}{2}(1 + \gamma_0)(A_{B^+} e^{-m_{B^+}t} + A_{B^-} e^{-m_{B^-}t}) + \frac{1}{2}(1 - \gamma_0)(A_{B^+} e^{-m_{B^+}(T-t)} + A_{B^-} e^{-m_{B^-}(T-t)}) + \dots, \quad (8)$$

where  $m_{B^+}$  and  $m_{B^-}$  refer to baryons with opposite intrinsic parity. In this paper only the lowest-lying meson and baryon states in each channel will be determined, since higher accuracy is needed to determine also the first excited states. In order to extract the hadron masses and

amplitudes, the correlation functions are fitted (at least in the Wilson fermion case) to a sum of two hyperbolic cosines for the mesons, and to two decaying exponentials for the baryons. The physical region of very small quark masses often has to be, at least with the presently avail-

able lattice sizes, obtained by extrapolation using the values of the hadron masses computed for larger quark masses: the smallest quark mass used in the present study corresponds to about 7 MeV. Results for even lighter quarks are then obtained by extrapolation. One should keep in mind that the *qualitative* behavior for small quark mass is presumably known from current algebra, just as the behavior for small  $g^2$  is known from perturbation theory, and one only needs to establish the necessary matching. This point will be discussed further below. For the light hadron masses, the simplest assumption is that they are given by expressions of the type

$$M^2 = M_0^2 + B_u m_u + B_d m_d + B_s m_s + C m^2, \quad (9)$$

where  $m$  is the average quark mass,  $B_u = \langle p | \bar{u}u | p \rangle$ , etc., and the label  $p$  denotes here the relevant state (pion, rho, proton, . . .). The constant  $C$  is expected to be 4 for mesons and 9 for baryons. When fermion polarization effects are included, it is known from chiral perturbation theory that pion emission and reabsorption gives rise to nonanalytic corrections of the type  $\sim n_f m^4 \ln m^2$  and  $\sim n_f m^{3/2}$ , with the second term absent for the pseudoscalar mesons, as a consequence of their pseudo-Goldstone nature.<sup>3</sup>

The finite spatial extent of the lattice poses a limit on the smallest pion mass that can be reached. In general one should adopt a conservative cut  $M_\pi L > 3$ , which will be roughly satisfied by the results presented below. This is equivalent to the requirement that the pion wave function should fit inside the space-time box, or that the masses in lattice units should lie between the ultraviolet and the infrared lattice cutoff  $\pi/La \ll M \ll \pi/a$ . For fixed gauge coupling, the hadron mass  $M$  can be made smaller only if  $L$ , the spatial extent of the box, is made larger. We partially circumvent this constraint here by studying smaller quark masses at stronger gauge coupling, and find surprisingly good agreement in the region where the data from the two couplings overlap. But we do not claim that the procedure used here is a substitute for studying even larger lattices. Similarly, finite-size effects coming from the gluons are expected to be contained: for periodic boundary conditions the finite-size corrections are exponentially in the linear spatial box size, with a decay length given by the inverse mass gap in the relevant channel. The mass gap has not been reliably measured when fermion loops are present, but one expects it to be relatively close to the result without loops, in physical units.

Finally the physical masses of the hadrons are obtained, by extrapolating the results obtained at finite coupling to the limit of zero coupling using the renormalization group. For finite  $g^2$  one expects from asymptotic freedom that for ratios for physical masses one has

$$\frac{M_a}{M_b} = C_{ab} [1 + O(\Lambda^2 a^2)] \quad (10)$$

and the lattice corrections should decrease rapidly for small  $g^2$ , since  $\Lambda a \sim \exp(-1/2\beta_0 g^2)$ . Alternatively, if physical quantities (renormalization-group invariants) are expressed in physical units such as MeV, then one ex-

pects to get the same results for different values of the gauge coupling. This indeed is what one finds for some of the quantities measured below.

### III. LATTICE RESULTS

Clearly one of the outstanding problems in the numerical study of QCD is the inclusion of fermion vacuum-polarization effects in a realistic study of the mass spectrum on a large lattice. The present study extends previous calculations with Wilson fermions done on a  $4 \times 4 \times 4 \times 16$  lattice, as well as on a  $10 \times 10 \times 10 \times 30$  lattice.<sup>8</sup> It confirms and substantially extends some of the qualitative features of dynamical fermion loop effects described there. In addition, some of the results presented in Ref. 8 have recently been confirmed by the independent computation of Ref. 12. Some of the newer results presented here have appeared in preliminary form in Ref. 13. The case of Susskind fermions<sup>11</sup> will not be discussed here, since the results with fermion loops there are more difficult to interpret due to the well-known fermion doubling problem and the difficulty that arises in deciding how many fermion flavors actually contribute to the loop effects for finite gauge coupling.<sup>7</sup> Here the aim is, on the one hand, to provide accurate data at a few values of the coupling constant (for the full theory on a reasonably large lattice), and at the same time gain some qualitative insight into the effects of the fermion loops on the hadron spectrum, the light-quark masses, and the QCD scaling parameter, as well as other quantities.

Details on the actual numerical simulation are briefly summarized as follows (further details can be found in Refs. 7 and 8). Two completely independent sets of configurations were generated on a  $10 \times 10 \times 10 \times 10$  lattice, one starting from a pure gauge configuration thermalized at  $\beta = 6/g^2 = 5.6$  ("hot start"), and another set from a pure gauge configuration thermalized at  $\beta = 0.6$  ("cold start"). The effects of the fermion determinant were then included with  $\beta = 5.4$  and  $n_f = 3$ , at five values of hopping parameter  $k = 0.156, 0.158, 0.160, 0.162, \text{ and } 0.163$ . 45 fermion propagators were then computed on the set of 45 configurations separated by 20 gauge iterations, and used in estimating the hadron masses. The so-obtained gauge configurations were then rethermalized with 300 gauge iterations at  $\beta = 5.3$  and  $n_f = 3$ , for four values of the hopping parameter  $k = 0.177, 0.178, 0.179, \text{ and } 0.180$ . Again 60 fermion propagators were then computed, on 12 configurations separated by 40 gauge iterations (5 propagator evaluations per configuration).

As pointed out before, when the fermion loop effects are taken into account two new "auxiliary" parameters need to be introduced (apart from the number of flavors  $n_f$  and  $k$  or the fermion mass  $m$ ): the step size used in the gauge updating  $\epsilon$  and the number of pseudofermion iterations needed to compute the fermion currents  $n_{\text{pf}}$ . In the limit that  $\epsilon$  goes to zero and  $n_{\text{pf}}$  goes to infinity, the algorithm becomes exact.<sup>19</sup> The pseudofermions needed in the gauge field updating were thermalized each time with 20+100 iterations (with 5 hits per site) at  $\beta = 5.4$  and 20+50 iterations at  $\beta = 5.3$ , and the step size

was chosen to be  $\epsilon=0.01$ .

For the gauge fields 4 hits were done at  $\beta=5.4$  and 8 hits for  $\beta=5.3$ . In the above range of parameters, the acceptance rate per link updating was about 73% for  $\epsilon=0.01$  and 81% for  $\epsilon=0.005$ . We also checked that the results were unchanged, within our errors, when the number of pseudofermion iterations was increased to 100 and 200. With the given fixed choice of parameters, we have found the pseudofermion algorithm to be quite stable, even at the smaller values of the quark masses. We do not of course claim that the method will not be affected by critical slowing down as the quark mass is reduced even further, but we were unable to do so here because of the smallness of our lattice.

The same set of gauge configurations were than also used to estimate the masses and wave functions of hadrons in the case of light sea versus heavy valence quarks, a situation that applies to the charmed-quark states such as the  $\eta_c$ , the  $J/\psi$ , and the  $D$ . In this last case a total of 20 propagators for each combination of the  $k$ 's listed in the tables were computed and averaged.

Thus the gauge configurations at different values of  $k$  can be taken as almost completely stastically independent, with *two* independent sets for each  $k$ . The lattices were then triplicated in the time direction to give a  $10 \times 10 \times 10 \times 30$  lattice, and the fermion propagators were subsequently evaluated (for different values of  $k$  or the quark mass) to high accuracy by a checkerboard Gaussian relaxation method with up to about 200 iterations. As in previous computations, both residual vector, individual matrix elements at the largest time separation, and hadron propagators were monitored to ensure accuracy in the matrix inversion for all values of the quark mass. If  $\chi$  denotes the sought-for-fermion propagator, we verified that for each inversion the relative residual vector always satisfied  $|M\chi - \delta_{x,x_0} \delta_{\alpha,\alpha_0} \delta_{a,a_0}|/|\chi| \leq 5 \times 10^{-3}$ . For each separate gauge configuration the location of the  $\delta$  function on the lattice was chosen randomly to decrease correlation effects. The accuracy in the matrix inversion is quite satisfactory, contributing to less than 1% of the error in the masses quoted (the uncertainty in the fit and the statistical fluctuation are by far the largest source of error). We also checked that, as in previous computations, the replication of the gauge configuration did not introduce any appreciable error in the hadron propagators. This is expected since the correlations are always much smaller here than the spatial lattice extent. Periodic boundary conditions were adopted for both the gauge fields and the fermions.

Statistical errors in the propagators and masses were estimated first by the usual binning procedure. Because of possible correlations in Monte Carlo time among different configurations, we also repeated the analysis with alternate or more configurations omitted, depending on the estimated correlation effects. In order to estimate the statistical correlations in the sample, we attempted to determine the autocorrelation effects (in Monte Carlo time) of the hadron propagators and masses using the standard methods. The autocorrelation time appears to be quite difficult to measure with our limited statistics, but we have obtained the following estimates regarding

the pion propagator at separation 10–15, where most of the fits are performed.

If the autocorrelation of the pion propagator is normalized to one at zero relative Monte Carlo time, then for  $\beta=5.3$  we obtain for the autocorrelation after 40 sweeps with  $\epsilon=0.01$  the values

$$k=0.177: 0.12, \quad k=0.178: 0.17,$$

$$k=0.179: 0.35, \quad k=0.180: 0.08.$$

After 80 sweeps the autocorrelation is difficult to measure because of our limited statistics, and for the same reason we quote the above values with no error at this point. For  $\beta=5.4$  we obtain for the same autocorrelation after 20 sweeps with  $\epsilon=0.01$  the values

$$k=0.156: 0.11, \quad k=0.158: 0.13,$$

$$k=0.160: 0.35,$$

$$k=0.162: 0.47, \quad k=0.163: 0.11,$$

with again significantly smaller values after 40 sweeps. Similar autocorrelations are found for the other propagators and/or states. Theoretical arguments can be given to suggest that autocorrelations should decay exponentially with a characteristic time related to the correlation length or inverse mass gap through a dynamical critical exponent. Furthermore they should increase for smaller quark masses, but our estimates at this point are not accurate enough to demonstrate this trend. Thus it appears that, for our choice of parameters and in particular  $\epsilon=0.01$ , after about 100 sweeps the correlations are contained (for smaller values of  $\epsilon$  this of course is no longer true and more sweeps will have to be used).

The availability of two completely statistically independent gauge configurations for each parameter combination, which could therefore be analyzed independently and compared, provided a further relatively stringent check on the errors. We also applied the "jack-knife" method (see second of Ref. 14 for a discussion) to the correlation functions to further check our errors, and found good agreement between the various error determinations. The correlation function fits were obtained using a nonlinear least-squares fit to the last four and five points ( $t=11-15$ ) using the Levenberg-Marquardt method. In addition, a double-exponential fit was also tried for all propagators, (*S*-wave states only) to check systematic effects. Errors were estimated by comparing the answer from the fits to the last three  $t$ -dependent mass estimates. Figure 1 illustrates a typical correlation function fit, together with the relative deviation.

The systematic uncertainty in the mass resulting from the fits and the statistical fluctuations in the correlation functions leads then to the errors quoted in Tables I–IV. It should be emphasized that since all hadron masses are extracted from the *same* set of fermion propagators (which are evaluated exactly on the same gauge configuration), the errors quoted are correlated among

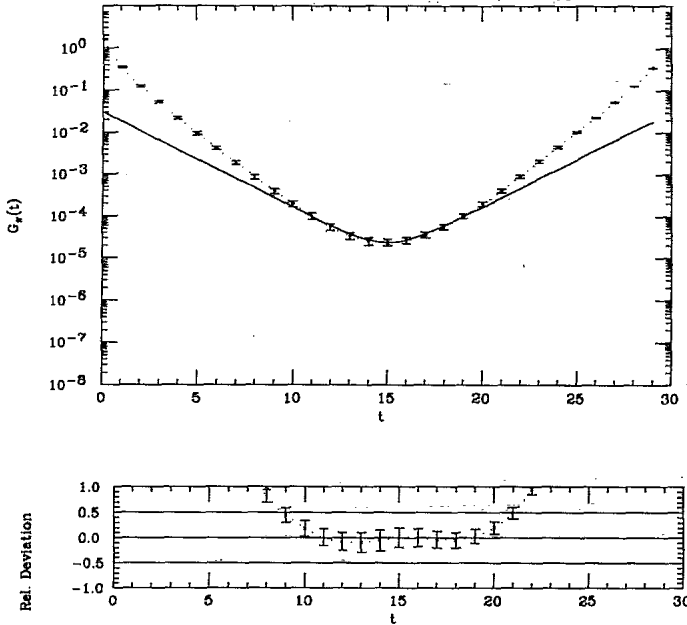


FIG. 1. The pion propagator for  $\beta=5.3$  and  $k=0.179$ . The average is over 70 quark propagators. Data in this and the following figures refer to  $\epsilon=0.01$ . The continuous line is obtained from the least-squares fit at large distances ( $t=11-15$ ), while the dotted line represents a cubic spline interpolation to the data. For this specific case, the pion mass is estimated at about  $0.52(3)$ , in lattice units.

different states for the same set of gauge configurations, and the spin splittings are determined more accurately than one might have expected from the uncertainty in the masses themselves. In the tables we have therefore presented also the values for the spin splittings directly.

Tables I–IV list the results for the hadron masses in lattice units. The symbols  $P$  and  $V$  refer to the pseudoscalar and vector mesons, respectively, while  $N$  and  $\Delta$  refer to the  $s=\frac{1}{2}$  and  $s=\frac{3}{2}$  baryons. The results for the pseudoscalar- and vector-meson masses are also displayed in Figs. 2(a), 2(b), and 3(b) (the lines in these figures are only intended as a guide to the eye). As mentioned before, in Tables I and II the mass of the “sea” quarks generating the vacuum-polarization effect is taken to be the same as the mass of the “valence” quarks that enters into the external propagators. The results therefore apply to the spectroscopy of light-quark ( $u, d, s$ ) bound states.

On the other hand, in Tables III and IV the sea quarks are taken to be lighter than the valence quarks. There the results of interest for the spectroscopy of heavier quark ( $c, b$ ) bound states, as will be discussed further below. As can be seen from the data, the fermion vacuum-polarization contribution of the light quarks significantly decreases the mass of the heavier-quark bound states. It can be interpreted as a consequence of the reduction of the overall QCD scale in units of the cutoff, caused by the light-quark loops and consistent with the continuum asymptotic-freedom prediction. As in the case of  $n_f=0$  (Ref. 5), the vector-meson mass and the baryon mass are not well fitted, for small quark

masses, by a linear function of  $1/k$  (or equivalently of the quark mass  $m$ ), whereas the quality of the fit improves when the masses squared are used (as in fact is quite clearly the case for the pion). Thus here all extrapolated values are quoted assuming linear behavior in  $1/k$  for all masses squared and mass squared differences.

#### IV. LIGHT HADRON MASSES

The inverse Wilson hopping parameter  $1/k$  is related to the quark mass. More precisely, one defines in the Wilson fermion case the lattice quark mass as

$$ma = \ln \left[ 1 + \frac{1}{2} \left( \frac{1}{k} - \frac{1}{k_c} \right) \right] \Bigg|_{k \sim k_c} \frac{1}{2} \left( \frac{1}{k} - \frac{1}{k_c} \right). \quad (11)$$

From the values in Tables I and II, one sees that the pseudoscalar-meson mass squared is well fitted by a linear function of  $1/k$  [see Figs. 2(a) and 2(b)]. One then finds, for small  $m$  and three light flavors,

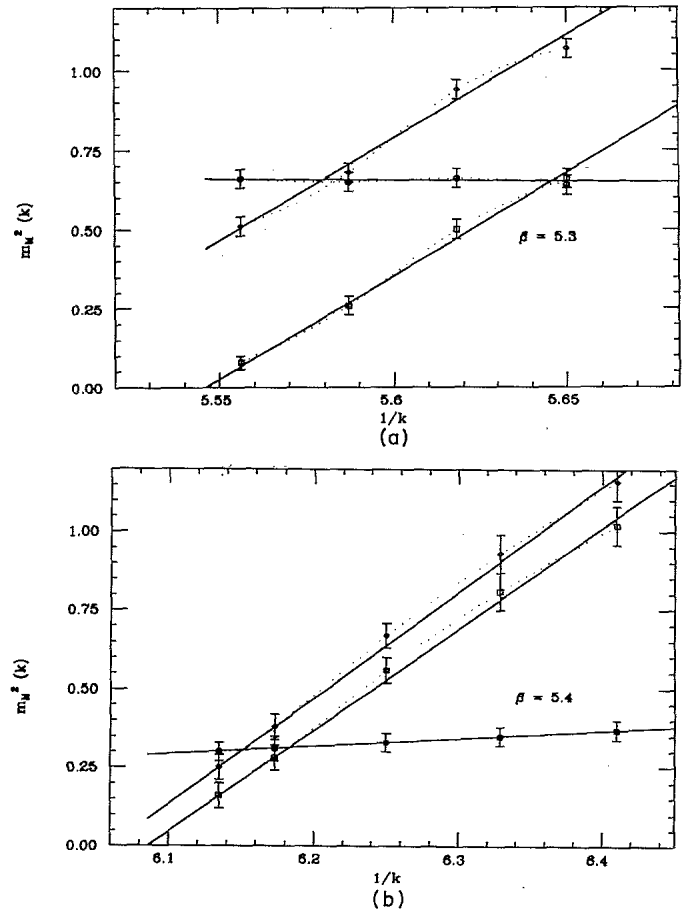


FIG. 2. (a) Pseudoscalar- and vector-meson mass squared in lattice units as a function of the parameter  $1/k$  (related to the bare quark mass) at  $g^2=1.132$  ( $\beta=5.3$ ) for Wilson fermions and  $n_f=3$ . Here  $m_{\text{sea}}=m_{\text{light}}$  always, and the data are from Table I. Squares: pseudoscalar-meson mass squared; diamonds: vector-meson mass squared; circles: square root of mass squared difference, as tabulated in Table I. The dotted line represents a cubic spline interpolation. Here and in the following the lines are only intended as a guide to the eye. (b) Same as in (a), but at  $g^2=1.111$  ( $\beta=5.4$ ) (data from Table II).

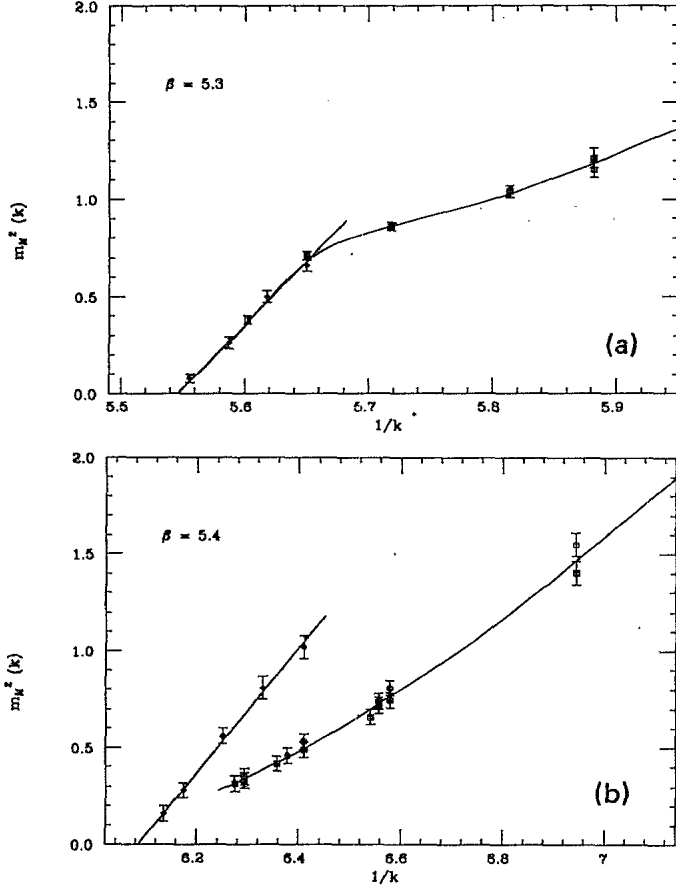


FIG. 3. (a) Pseudoscalar-meson mass for  $\beta=5.3$  [same as in Fig. 2(a)], but now combining data points for  $m_{\text{sea}} = m_{\text{valence}}$  (diamonds) with points for which  $m_{\text{sea}} \ll m_{\text{valence}}$  (squares along lower line). Both the case of equal-mass and unequal-mass quarks are displayed, and  $1/k = (1/k_1 + 1/k_2)/2$  here. Note that all points for  $m_{\text{sea}} \ll m_{\text{valence}}$  lie close to one single curve. The squares correspond to the choice  $k_{\text{sea}} = 0.180$ . The data are from Tables I and III. (b) Pseudoscalar-meson mass for  $\beta=5.4$  [otherwise the same as in Fig. 2(b)], again combining data points for  $m_{\text{sea}} = m_{\text{valence}}$  (diamonds) with points for which  $m_{\text{sea}} \ll m_{\text{valence}}$  (circles and squares along lower curve). Both the case of equal-mass and unequal-mass quarks are displayed, and  $1/k = (1/k_1 + 1/k_2)/2$  here. Note that all points for  $m_{\text{sea}} \ll m_{\text{valence}}$  lie close to one single curve. The circles correspond to  $k_{\text{sea}} = 0.162$  and the squares to  $k_{\text{sea}} = 0.163$ . The data are from Tables II and IV.

$$M_P^2 = (A_P a^{-1})m + O(m^2) \quad (12)$$

with  $A_P = 12.6(10)$  and  $6.5(6)$  at  $\beta=5.3$  and  $\beta=5.4$ , respectively. The slopes are determined here in the case of  $m_{\text{sea}} = m_{\text{valence}}$ . In the graphs a cubic spline interpolation is also presented for comparison to the simplest, but possibly biased, straight-line fit.

The lattice spacing can be determined, for example, from the  $\rho$  (vector-meson) mass. One way of doing it is to compute the quantity  $(M_V^2 - M_P^2)^{1/2}$  and extrapolate it to the chiral limit. From phenomenology one knows that this quantity is almost constant in going from the  $\rho, K$  to the  $J/\psi$ . Indeed the lattice QCD results seem to reproduce this trend. One concludes that the lattice spacing in the Wilson fermion case for  $n_f=3$  is much smaller than

for  $n_f=0$  (Ref. 8):

$$\begin{aligned} a_W^{-1}(\beta=5.3, n_f=3) &= 1130(50) \text{ MeV}, \\ a_W^{-1}(\beta=5.4, n_f=3) &= 2600(200) \text{ MeV}, \\ a_W^{-1}(\beta=5.4, n_f=0) &= 980(100) \text{ MeV}, \\ a_W^{-1}(\beta=6.0, n_f=0) &= 1950(200) \text{ MeV}. \end{aligned} \quad (13)$$

All the estimates with fermion loops refer to  $\epsilon=0.01$ , as mentioned before. Alternatively one can fix the lattice spacing by extrapolating  $M_V$  linearly in the quark mass (for small mass), obtaining a lattice spacing of about 1100 and 2100 MeV at  $\beta=5.3$  and  $5.4$ , respectively. In the following the previous values will be used, but a certain extrapolation ambiguity has to be kept in mind. Of course on a larger lattice it should be possible to go to a smaller value of the quark mass and thus substantially reduce the uncertainty.

Thus the lightest pseudoscalar-meson mass considered here is about 330 MeV at  $\beta=5.3$ , while the largest mass is about 2600 MeV at  $\beta=5.4$ . The lattice spacing itself is about 0.18 fm at  $\beta=5.3$  and 0.08 fm at  $\beta=5.4$ , while the linear lattice size is consequently 10 times larger.

When comparing the results at  $\beta=5.3$  with the ones at  $\beta=5.4$ , one notices that the change in the lattice spacing  $a_W$  roughly compensates for the change in the lattice pion slope  $A_P$ . As a consequence the slope in physical units is about the same for the two values of the gauge coupling considered here. It should be added that one unsatisfactory feature of the Wilson fermion formulation is the fact that  $k_c$  is quite sensitive to  $\epsilon$  and that the masses in lattice units are expected to change as  $\epsilon$  is decreased further. On the other hand the precise value of  $k_c$  is not related to any observable (the light-quark masses are, for example, determined from the slope in  $1/k$ ) and different (small) values of  $\epsilon$  appear to give the same values for physical dimensionless ratios, as was also observed in Ref. 12.

In Figs. 3(a) and 3(b) similar results for the pseudoscalar are displayed, including values for the case of heavy-light and heavy-quark systems with light sea quarks (applicable to the case of the  $\bar{c}u$  and  $\bar{c}c$  pseudoscalars, respectively, with light  $u$ -,  $d$ -,  $s$ -quark loop contributions). In Fig. 4 the same computed values are redisplayed, combining  $\beta=5.3$  and  $\beta=5.4$ , in *physical units* which are derived utilizing the above quoted values for the cutoff  $a^{-1}$  in MeV.

The effect of vacuum-polarization loops introduces logarithmic corrections to the simple formula of Eq. (12). In the chiral limit the leading nonanalytic correction to the pion mass is given by chiral perturbation theory<sup>15,16</sup>

$$m_\pi^2 = \sigma_\pi \left[ 1 + \frac{1}{32\pi^2 f_\pi^2} \left[ \sigma_\pi \ln \frac{\sigma_\pi}{\mu^2} - \frac{1}{3} \sigma_\eta \ln \frac{\sigma_\eta}{\mu^2} \right] \right] \quad (14)$$

with

$$\begin{aligned} \sigma_\pi &= \frac{1}{2}(m_u + m_d) \langle \pi^+ | \bar{u}u | \pi^+ \rangle, \\ \sigma_K &= \frac{1}{2}(m_u + m_s) \langle K^+ | \bar{u}u | K^+ \rangle, \\ \sigma_\eta &= \frac{1}{3}(4\sigma_K - \sigma_\pi), \end{aligned} \quad (15)$$

TABLE I. Hadron masses ( $S$  waves) in lattice units at  $g^2=1.132$  ( $\beta=5.3$ ) for Wilson fermions and  $n_f=3$ . Here  $\epsilon=0.01$  and  $m_{\text{sea}}=m_{\text{valence}}$  always. Extrapolations are discussed in the text.

$k$	0.177	0.178	0.179	0.180	0.1804(2)
$m$					0.000
$M_P$	0.82(2)	0.69(3)	0.52(3)	0.29(3)	0.00
$M_V$	1.04(3)	0.95(4)	0.84(4)	0.73(4)	
$(M_V^2 - M_P^2)^{1/2}$	0.64(3)	0.65(3)	0.66(3)	0.67(3)	0.67(3)
$M_N$	1.53(7)	1.37(11)	1.18(12)	0.97(9)	
$(M_N^2 - 2.8M_P^2)^{1/2}$	0.68(9)	0.73(13)	0.80(12)	0.84(12)	0.86(9)
$M_N/M_V$	1.47(11)	1.44(19)	1.40(23)	1.33(21)	
$M_\Delta$	1.66(9)	1.52(13)	1.37(13)	1.20(11)	
$(M_\Delta^2 - M_N^2)^{1/2}$	0.65(7)	0.67(6)	0.69(5)	0.71(6)	0.71(5)
$f_P$	0.18(2)	0.17(2)	0.15(2)	0.12(4)	
$f_P/M_V$	0.17(2)	0.18(2)	0.18(2)	0.16(4)	0.17(2)

TABLE II. Hadron masses ( $S$  waves) in lattice units at  $g^2=1.111$  ( $\beta=5.4$ ) for Wilson fermions and  $n_f=3$ . As in Table I,  $\epsilon=0.01$  and  $m_{\text{sea}}=m_{\text{valence}}$  always. Extrapolations are discussed in the text.

$k$	0.156	0.158	0.160	0.162	0.163	0.1643(3)
$m$						0.00
$M_P$	1.01(5)	0.90(3)	0.75(2)	0.52(3)	0.40(4)	0.00
$M_V$	1.08(5)	0.97(3)	0.82(3)	0.61(3)	0.50(5)	
$(M_V^2 - M_P^2)^{1/2}$	0.37(3)	0.35(3)	0.33(3)	0.31(4)	0.30(3)	0.29(2)
$M_N$	1.71(9)	1.54(6)	1.30(4)	0.93(7)	0.76(9)	
$(M_N^2 - 2.8M_P^2)^{1/2}$	0.27(5)	0.31(6)	0.33(5)	0.34(5)	0.35(7)	0.36(5)
$M_N/M_V$	1.58(17)	1.59(11)	1.59(11)	1.52(19)	1.52(37)	
$M_\Delta$	1.74(10)	1.58(7)	1.34(5)	0.99(8)	0.83(11)	
$(M_\Delta^2 - M_N^2)^{1/2}$	0.32(5)	0.35(4)	0.33(5)	0.33(4)	0.33(6)	0.33(4)
$f_P$	0.14(2)	0.12(1)	0.09(1)	0.06(1)	0.05(1)	
$f_P/M_V$	0.13(2)	0.12(1)	0.11(1)	0.10(1)	0.10(1)	0.11(1)

TABLE III. Masses of light-heavy- (first four columns) and heavy-heavy-quark mesons (last four columns, \*) (all  $S$  waves) in lattice units at  $g^2=1.132$  ( $\beta=5.3$ ) for Wilson fermions and  $n_f=3$ , and  $\epsilon=0.01$ . Here  $m_{\text{sea}}=m_{\text{light}}$  in the light-heavy-quark bound-state case.  $\bar{m}$  is the quark mass corresponding to  $\bar{k}=(1/k_1+1/k_2)/2$ , with 1 and 2 referring to the two valence quarks.

$k_{\text{light}}=k_{\text{sea}}=0.180$					
$k_{\text{heavy}}$	0.160	0.165	0.170	0.177	
$\bar{m}$	0.165	0.123	0.083	0.028	
$M_P$	1.08(2)	1.01(2)	0.93(2)	0.64(3)	
$M_V$	1.22(3)	1.17(4)	1.12(3)	0.92(4)	
$(M_V^2 - M_P^2)^{1/2}$	0.57(2)	0.60(3)	0.62(2)	0.66(3)	
$f_P$	0.22(2)	0.19(2)	0.19(2)	0.16(2)	
$f_P/M_V$	0.18(2)	0.16(2)	0.17(2)	0.17(2)	
$k_{\text{sea}}=0.180$					
$k_{\text{heavy}}$	0.160*	0.165*	0.170*	0.177*	
$\bar{m}$	0.302	0.229	0.155	0.050	
$M_P$	1.35(2)	1.21(2)	1.05(2)	0.84(2)	
$M_V$	1.43(2)	1.32(3)	1.20(3)	1.05(3)	
$(M_V^2 - M_P^2)^{1/2}$	0.47(2)	0.52(3)	0.58(3)	0.63(3)	
$f_P$	0.24(2)	0.22(2)	0.17(2)	0.16(2)	
$f_P/M_V$	0.17(2)	0.17(2)	0.14(2)	0.15(2)	

TABLE IV. Masses of light-heavy- (first three columns) and heavy-heavy-quark mesons (last three columns, \*) (all  $S$  waves) in lattice units at  $g^2=1.111$  ( $\beta=5.4$ ) for Wilson fermions and  $n_f=3$ , and  $\epsilon=0.01$ . Here  $m_{\text{sea}}=m_{\text{light}}$  in the light-heavy-quark bound-state case.

$k_{\text{light}}=k_{\text{sea}}=0.162$						
$k_{\text{heavy}}$	0.144	0.152	0.156	0.144*	0.152*	0.156*
$\bar{m}$	0.212	0.135	0.098	0.357	0.220	0.150
$M_P$	0.85(4)	0.66(3)	0.57(3)	1.24(3)	0.89(3)	0.71(3)
$M_V$	0.88(5)	0.70(3)	0.61(4)	1.26(4)	0.92(4)	0.74(4)
$(M_V^2 - M_P^2)^{1/2}$	0.24(2)	0.23(2)	0.22(2)	0.23(3)	0.24(3)	0.22(2)
$f_P$	0.075(7)	0.069(7)	0.068(7)	0.132(6)	0.088(5)	0.082(7)
$f_P/M_V$	0.085(7)	0.098(7)	0.111(7)	0.105(6)	0.096(5)	0.111(7)
$k_{\text{light}}=k_{\text{sea}}=0.163$						
$k_{\text{heavy}}$	0.144	0.152	0.156	0.144*	0.152*	0.156*
$\bar{m}$	0.204	0.127	0.089	0.357	0.220	0.150
$M_P$	0.81(3)	0.65(3)	0.56(3)	1.19(3)	0.87(3)	0.71(3)
$M_V$	0.85(4)	0.70(4)	0.62(4)	1.21(4)	0.91(4)	0.75(4)
$(M_V^2 - M_P^2)^{1/2}$	0.27(2)	0.27(2)	0.27(2)	0.24(3)	0.26(3)	0.25(2)
$f_P$	0.077(6)	0.072(6)	0.069(5)	0.120(7)	0.093(5)	0.088(6)
$f_P/M_V$	0.091(7)	0.103(7)	0.113(7)	0.099(8)	0.102(5)	0.117(7)

and all matrix elements are evaluated for renormalized operators in the chirally symmetric limit of the QCD Hamiltonian.  $\sigma_P$  is essentially equal to the quantity  $A_P a^{-1} m$  defined above, expressed in physical units. Similar formulas hold for the  $K$  and  $\eta$  mesons.<sup>16</sup> While the coefficient of the leading nonanalytical contribution to the pseudoscalar mesons is fixed by chiral perturbation theory, the parameter  $\mu$  is not, and requires a nonperturbative calculation. It is difficult to see such a small logarithmic correction in the lattice QCD data, which has large statistical errors as well as errors coming from the approximate nature of the fermion algorithm. But from the results for  $m_q < 60$  MeV one obtains consistency with the above corrections provided that one has approximately  $\mu \approx 900$  MeV. If the slope is allowed to vary slightly in the fit, the estimate for the scale in the logarithm remains almost unchanged. More accurate and reliable data is clearly needed though to determine this small correction more precisely.

Equivalently, one can say that the argument of the logarithm is close to one for a quark mass  $m \approx 50$  MeV, which, as will be shown below, corresponds roughly to the strange-quark mass. Thus perhaps the correction due to the logarithm is quite small and does not significantly affect at this point the estimates for the pion slope given above. Note that the smallness of this correction could provide an indirect evidence for chiral-symmetry restoration with the Wilson fermions [at strong coupling the pion-scattering amplitude does not vanish for zero momentum, and the current-algebra low-energy theorems for pion scattering, implicitly assumed in the derivation of Eq. (14), are not valid].

Tables I and II list also the values for the nucleon mass and the quantity  $(M_N^2 - 2.8M_P^2)^{1/2}$ , where  $M_N$  and  $M_P$  are the nucleon and pseudoscalar-meson masses, respectively. In the chiral limit this last quantity still reduces to the nucleon mass. The reason for this specific choice is

twofold. Firstly the nucleon mass is rapidly increasing as a function of the quark mass and therefore difficult to determine for  $m_q=0$ . By subtracting a multiple of the pion mass one obtains a quantity which is less rapidly varying. Secondly the two masses are correlated and the above difference is computed more accurately than the individual errors might suggest (the same procedure is quite reliable for obtaining the  $\pi$ - $\rho$  splitting, as discussed above). As a function of Euclidean distance  $t$ , it is a rapidly decreasing function. The factor 2.8 is the approximately determined ratio between pion and nucleon slopes. It is about the same with and without quark loops, both for Wilson and Susskind fermions.<sup>5,8</sup> The following estimates would not change if that number was taken to be say 3.0 instead. In fact from the data one sees that the above-mentioned difference is not quite constant (it slowly increases in the chiral limit). One way of estimating the systematic error is to compute the distance-dependent ratio (of spin splittings)

$$R(t) = [M_N^2(t) - 2.8M_P^2(t)]^{1/2} [M_V^2(t) - M_P^2(t)]^{1/2}.$$

Again this procedure exploits the fact that the quantities in the numerator and in the denominator are statistically correlated. The physical mass of the nucleon (we do not distinguish proton and neutron here) is then estimated using this first procedure at

$$\begin{aligned} M_N &= 970(140) \text{ MeV} \quad (\beta=5.3), \\ M_N &= 970(210) \text{ MeV} \quad (\beta=5.4), \end{aligned} \quad (16)$$

which includes the uncertainty in the value of the lattice spacing and should be compared with the experimental value of 940 MeV. One should add though that in the case of  $\beta=5.4$  a substantial extrapolation in the quark mass has been done.

The above values and errors refer to the case in which the nucleon mass squared is assumed to be linear in the



quark mass, as suggested in Ref. 3. Alternatively one might try to extrapolate the nucleon mass itself in the quark mass. From the data in Tables I and II one then obtains from the two smallest values of the quark mass, by linear extrapolation, the estimates

$$\begin{aligned} M_N &= 980(180) \text{ MeV} \quad (\beta=5.3), \\ M_N &= 1130(200) \text{ MeV} \quad (\beta=5.4). \end{aligned} \quad (17)$$

(If all the data points had been used in the fit, the extrapolated result would have been still higher.) Finally, still regarding the nucleon, one can try to determine instead the dimensionless ratio  $M_N/M_V$  in the chiral limit. Again from the data in the table one finds that this ratio (which has large errors) tends toward the right value at

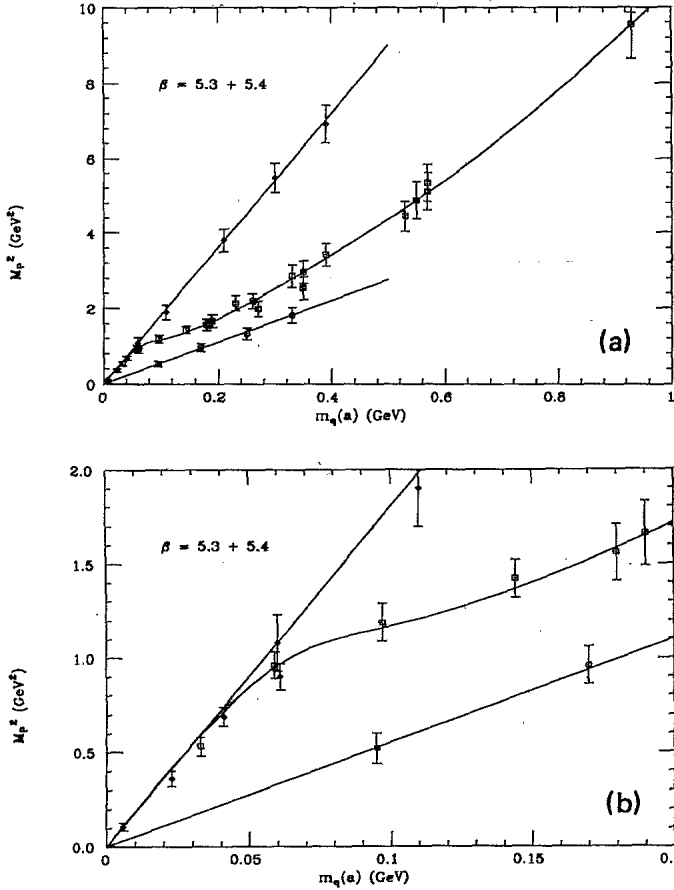


FIG. 4. (a) Pseudoscalar-meson mass in physical units (GeV) versus the (valence-) quark mass, also in physical units. The scale (here given by the lattice spacing  $a^{-1}$ ) is obtained from the physical  $\rho$ - $\pi$  mass splitting. Both full data sets for  $\beta=5.3$  and  $\beta=5.4$  are combined; the good overlap between the two data sets should be noted. In the continuum one expects a universal curve (up to a small anomalous dimension factor correction for the quark mass). Data points for  $m_{\text{sea}} = m_{\text{valence}}$  are indicated by diamonds, while points for which  $m_{\text{sea}} \ll m_{\text{valence}}$  are indicated by squares. Both the case of equal- and unequal-mass quarks are displayed here together, as in Figs. 2(b) and 2(c). The circles correspond to  $\beta=6.0$  and  $n_f=0$  (no fermion loop effects). (b) Enlarged view of the small quark mass region displayed in the previous figure.

$\beta=5.3$  [ $\approx 1.3(2)$ ], but is stable at 1.5 at the weaker coupling  $\beta=5.4$ . This situation is quite unsatisfactory, but might just reflect the fact that this ratio is more rapidly varying, and that in the latter case the quark mass is not small enough to see any decrease. In any case the quality of the data for the nucleon does not allow one to discriminate between the various extrapolation procedures. Of course on a larger lattice it should be possible to go to a smaller value of the quark mass and thus substantially reduce the uncertainty.

The accuracy of the results for the nucleon is insufficient at this point to detect the leading nonanalytic corrections in the quark mass which are presumably due to the surrounding pion cloud, as discussed in Refs. 3 and 16. This in spite of the fact that the correction is believed to be larger in this case, due to the nonvanishing (in fact quite large) pion-nucleon coupling in the chiral limit: following Ref. 3 the effects of the pion cloud contribute a nonanalytic  $m^{3/2}$  correction in the nucleon case

$$M_N^2 = M_0^2 + Bm - \frac{3g_A^2 M_0}{16\pi f_\pi^2} m^3 + \dots, \quad (18)$$

where we have set  $m = (m_u + m_d)/2$  and

$$B = 3 \langle p | \bar{d}d | p \rangle = \frac{3}{2} \langle p | \bar{u}u | p \rangle, \quad (19)$$

and assumed  $m_u \approx m_d$ . For the lightest-quark mass considered here, the correction is comparable to the quoted error in the nucleon mass. Also it is unclear at this point what the size of the higher-order corrections in this model is.

Another quantity of interest that can be, in principle, computed with relative ease is the strangeness content of the proton  $\langle p | \bar{s}s | p \rangle$ . It can be derived from the proton-mass slope versus the quark mass. Since in the numerical simulation the sea- and valence-quark masses can be varied independently, two independent slopes can be determined. The hadron masses are actually computed as a function of  $k$ , but  $\partial/\partial m_q = \frac{1}{2} \partial/\partial(1/k)$  for small  $m$ . One finds, for a gauge coupling  $\beta=5.3$ ,

$$\begin{aligned} \frac{\partial M_p^2}{\partial m_{\text{sea}}} &= 21.3(4.2)a^{-1}, \\ \frac{\partial M_p^2}{\partial m_{\text{valence}}} &= 14.3(2.7)a^{-1}, \end{aligned} \quad (20)$$

and for  $\beta=5.4$ ,

$$\begin{aligned} \frac{\partial M_p^2}{\partial m_{\text{sea}}} &= 9.2(2.2)a^{-1}, \\ \frac{\partial M_p^2}{\partial m_{\text{valence}}} &= 8.7(1.2)a^{-1}. \end{aligned} \quad (21)$$

The strangeness contribution to the proton mass comes entirely from the sea-quark effects, and one obtains for the dimensionless fraction

$$\frac{\langle p | \bar{s}s | p \rangle}{\langle p | (\bar{u}u + \bar{d}d + \bar{s}s) | p \rangle} \quad (22)$$

the values 0.20(5) and 0.17(5) at  $\beta=5.3$  and  $\beta=5.4$ , re-

spectively. The first estimate is more reliable since it corresponds to much smaller quark masses, as described above, and the second value should only be considered for reference, given the substantial quark mass extrapolation involved. The lattice QCD result can then be compared to the indirect experimental estimate of  $\approx 0.21$ , and to the Skyrme-model result  $\frac{7}{30} = 0.23$  (Ref. 14). But due to the many sources of uncertainty in the fermion-loop calculation as a whole, the lattice results can only be regarded as preliminary and qualitative at this point.

Turning to the other baryons, the  $\Delta$ -nucleon spin splitting is computed as

$$\begin{aligned} M_{\Delta}^2 - M_N^2 &= [800(100) \text{ MeV}]^2 \quad (\beta=5.3), \\ M_{\Delta}^2 - M_N^2 &= [860(180) \text{ MeV}]^2 \quad (\beta=5.4), \end{aligned} \quad (23)$$

again in good agreement with the experimental value of 805 MeV. Contrary to the situation in the strong-coupling region, there is *no* indication here that the spin splittings are smaller than the experimental values.

The hadron mass values quoted are in qualitative agreement with the experimental values, but the errors are unfortunately still quite large (and substantially worse than in the quenched approximation), and the extrapolation to small quark mass is still to a certain extent a question of subjective judgment. We believe that we have shown here that under reasonable assumptions no gross inconsistency with the observed spectrum has been found yet.

## V. MESON DECAY CONSTANTS

The meson decay constants are obtained from the amplitude of the large-distance decay of the relevant Euclidean correlation function and provide direct information on the decay widths of the mesons. Earlier computations of these constants were incomplete, in the sense that they did not include the effects of fermion loops (see, for example, Ref. 17 and references therein). It is of some interest to see whether the results with fermion loops are substantially different from the ones without loop effects. We will find indications that this is not the case, within the accuracy of the present computation. Define the pseudoscalar decay constant  $f_P$  by

$$\sqrt{2} f_P M_P = \langle 0 | \bar{\psi}_1 \gamma_5 \gamma_0 \psi_2 | P \rangle. \quad (24)$$

An alternative procedure would be to define  $f_P$  using the PCAC (partial conservation of axial-vector current) relation

$$\sqrt{2} f_P M_P^2 = (m_1 + m_2) \langle 0 | \bar{\psi}_1 \gamma_5 \psi_2 | P \rangle \quad (25)$$

but we have chosen not to do so here, even though the results for small quark masses would agree to a few percent, or within the errors. In a nonrelativistic potential model  $f_P$  is related to the modulus of the pseudoscalar-meson wave function at the origin

$$|\psi(0)| = \left[ \frac{M}{6} \right]^{1/2} f_P \quad (26)$$

and the experimentally measurable two-photon decay

width/rate is then given by

$$\Gamma(P \rightarrow \gamma\gamma) = \frac{48\pi\alpha^2}{M_P^2} \langle Q^2 \rangle |\psi(0)|^2. \quad (27)$$

In a general nonrelativistic potential model with potential  $V(r) = br^\sigma$ , the  $S$ -wave meson wave function at the origin can be obtained from Schrödinger's equation

$$|\psi(0)|^2 = cb^{3/(2+\sigma)} \mu^{3/(2+\sigma)}, \quad (28)$$

where  $c$  is a numeric constant and  $\mu$  is the reduced mass

$$\frac{1}{\mu} = \frac{1}{m_Q} + \frac{1}{m_q} \quad (29)$$

with  $m_Q$  and  $m_q$  the mass of the heavy and light quarks, respectively. In the following we will assume that, for heavy pseudoscalar mesons, the above result is qualitatively correct as far as the dependence of  $f_P$  on the *heavy* quark is concerned. It is clearly inadequate as far as the dependence on the *light*-quark mass is concerned, a situation which is usually ascribed to the fact that relativistic and nonperturbative effects presumably play an important role in the dynamics of the bound state. The values for the pseudoscalar decay constants  $f_P$  are reported in Tables I–IV. Actually the ratios of the decay constant over the vector-meson mass,  $f_P/M_V$ , are given, since they represent dimensionless numbers and are therefore less sensitive to fluctuations in the overall scale determined by the cutoff  $a^{-1}$ . The use of  $M_V$ , instead of  $M_P$ , is motivated by the fact that the latter choice, while adequate for heavy quarks, would lead to a divergent ratio in the chiral limit.

Results are available both for the case  $m_{\text{sea}} = m_{\text{valence}}$  (Tables I and II) and  $m_{\text{sea}} \ll m_{\text{valence}}$  (Tables III and IV). In the latter case results are given both for mesons composed of quarks of equal mass, as well as for mesons made out of quarks with unequal mass. To give an idea of the quark mass range involved, as can be seen from the values quoted in Table III ( $\beta=5.3$ ) and in Table IV ( $\beta=5.4$ ), in the unequal-mass case the (lattice) light-quark mass is about 70 MeV ( $k=0.163$ ) or 125 MeV ( $k=0.162$ ) for  $\beta=5.4$ , and about 7 MeV ( $k=0.180$ ) for  $\beta=5.3$ . Similarly, the heavy quark weighs at most about 1060 MeV ( $k=0.144$ ,  $\beta=5.4$ ). We shall restrict here the discussion about the decay constant results to the case  $\beta=5.4$ , since the values for  $f_P$  at  $\beta=5.3$  are clearly too large, a situation that is encountered also in the case  $n_f=0$  for too strong coupling. It can be ascribed to the fact that the wave function is more sensitive than the mass to finite-lattice-cutoff effects, which are expected to be larger at smaller  $\beta$ .

At first it would seem that one needs to extrapolate in the mass of the light quark in order to extract a value for  $f_P$ , say in the case of the  $D$  ( $\bar{c}u$ ) meson, since the  $u$  quark is very light. In order to do so, two values for the light-quark mass (related to  $k_{\text{light}}$ ) were considered in Table IV. But in spite of the light-quark mass decreasing by about a factor of 2, the values for the decay constant  $f_P$  remain about the same (within the errors), indicating the *absence* of a rapid change when the light-quark mass goes

to zero, at least within the framework of the present computation. From the data for  $f_P/m_V$  given in Table IV ( $\beta=5.4$ ) and Fig. 5, one obtains, therefore, for the pseudoscalar mesons the continuum estimates

$$\begin{aligned} f_\pi &= 100(15) \text{ MeV}, & f_K &= 110(15) \text{ MeV}, \\ f_D &= 200(20) \text{ MeV}, & f_{\eta_c} &= 320(25) \text{ MeV}, \end{aligned} \quad (30)$$

which are in good agreement, in the known cases ( $f_\pi, f_K$ ), with experiment. (With the above definition, the experimental value of  $f_\pi=93.5$  MeV.) In the above estimates we have included a perturbative correction relating the lattice decay constants to the continuum ones,  $f_P^c = Z_P f_P^{\text{latt}}$  with  $Z_P=0.84$ . This finite-renormalization factor arises because of the explicit chiral-symmetry breaking inherent in the Wilson fermion formulation.<sup>18</sup> Indeed these constants have also been evaluated nonperturbatively by looking at an appropriate three-point function (second of Ref. 5), but only in the case  $n_f=0$  and for a different gauge coupling. Since in the pseudoscalar case the difference between the perturbative answer and the nonperturbative one is comparable to our errors, we will not include further discussion of it in the following, and use the perturbative estimate, but keep in mind that our estimate might still be a few (10–20%) too high. The dependence of  $f_P$  on the meson or quark mass appears to be in good agreement with the few known experimental values (see Fig. 5). The vector-meson decay constant were also computed ( $f_\rho, f_\phi, f_\psi$ ) and, once the perturbative lattice correction is again included (the local vector bilinear fermion operator was used in the computation), one finds values that are about 15% higher than the experimental numbers, but with the correct trend as a function of the quark mass. This can provide a further check on the systematic effects that could affect the quoted re-

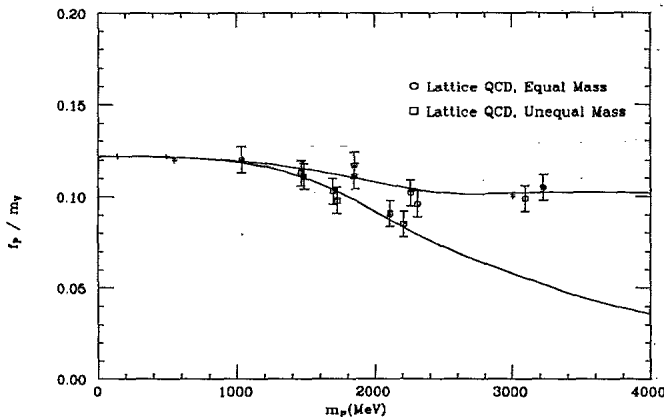


FIG. 5. The dimensionless ratio  $f_P/m_V$ , where  $f_P$  is the pseudoscalar decay constants and  $M_V$  the corresponding vector-meson mass, as a function of  $M_P$ , the pseudoscalar-meson mass, in physical units. Except for the smallest mass value, the data points were obtained in the case  $m_{\text{sea}} \ll m_{\text{valence}}$  (see Table IV). In the heavy-light-quark meson case (“unequal mass”), all points appear to lie close to one universal curve. The crosses correspond to the experimental values for the  $\pi$ ,  $K$ ,  $\eta$ , and  $\eta_c$  mesons.

sults. On the other hand the errors in this case are larger, and higher statistics would be needed to draw definite conclusions. In reference to the experimental situation, in the case of  $f_D$  the above value is just below the bound of  $f_D < 290$  MeV (90% C.L.) obtained by Mark III (Ref. 2). The above computation indicates that perhaps the decay  $D^+ \rightarrow \mu^+ \nu_\mu$  should be seen soon.

For heavier quarks (i.e., the  $b$ ) the decay constants have to be obtained here by extrapolation. To accurately study the  $b$  mesons a smaller lattice spacing is needed, which requires therefore a weaker gauge coupling and a larger lattice (such that the mass of the state is smaller than the ultraviolet cutoff  $a^{-1}$ ). Alternatively one could consider (in the heavy-light-quark bound-state case) the “hydrogenic” case separately, but these last two approaches are beyond the scope of this work. By looking at the data in Fig. 5 one notices though that the decay constants in the equal and unequal cases behave indeed differently for larger quark mass, as suggested by the simple nonrelativistic potential model result. From the data one estimates for large meson masses, in the heavy-light ( $h-l$ ) and heavy-heavy case ( $h-h$ ), respectively,

$$\begin{aligned} f_P^{(h-l)} &\sim [430(40) \text{ MeV}]^{3/2} M_V^{-1/2}, \\ f_P^{(h-h)} &\sim [0.102(10)] M_V, \end{aligned} \quad (31)$$

where  $M_V$  is the vector-meson mass; both of these curves are shown in Fig. 5 for large quark mass. Therefore the best lattice QCD estimate at this point would be

$$f_B = 130(20) \text{ MeV}, \quad f_{\eta_b} = 950(90) \text{ MeV}. \quad (32)$$

Note also that an additional (small) error is being made here since the number of light-quark flavors for the  $B$  system is presumably closer to four ( $u$ -,  $d$ -,  $s$ -,  $c$ -quark loops) than to three.

In QCD the nonrelativistic prediction [Eq. (24)] is actually modified, for heavy-light systems, by logarithms involving the mass of the heavy quark.<sup>19</sup> To leading order in  $\alpha_s$  one has

$$\frac{f(m_{Q'})}{f(m_Q)} = \left[ \frac{m_Q}{m_{Q'}} \right]^{1/2} \left[ \frac{\alpha_s(m_Q)}{\alpha_s(m_{Q'})} \right]^{-6/(33-2n_f)} \quad (33)$$

This relationship therefore suggests that one should try to determine instead the quantity  $\tilde{f}_P$  in the equation

$$f_P(m_Q) = \tilde{f}_P(m_Q)^{-1/2} \left[ \ln \frac{m_Q}{\Lambda_{\overline{\text{MS}}} } \right]^{-6/(33-2n_f)} \quad (34)$$

with  $\Lambda_{\overline{\text{MS}}} = 125(10)$  MeV for  $n_f=3$  (Ref. 8) where  $\overline{\text{MS}}$  denotes the modified minimal subtraction scheme. Depending on the choice for  $m_Q$  (“constituent-” or “current-algebra” quark mass), one obtains from the computed values in the  $D$ -meson region  $\tilde{f}_P^{1/3} \approx 350(50)$  MeV and therefore again about  $f_B = 130(20)$  MeV. The relative “insensitivity” of  $f_B$  to the logarithmic correction can be ascribed to the fact that the theoretical estimates have large errors, and that the logarithm is slowly varying in the region considered. It will be interesting to see how close these and future more refined estimates for

$f_D$ ,  $f_B$ , and  $f_{\eta_b}$ , are to the (yet to be determined) experimental numbers.

## VI. QUARK MASSES

The (lattice) quark mass  $m(a)$  is obtained indirectly from the functional dependence of the pseudoscalar-meson mass (or vector-meson mass) on the former, as defined in Eq. (12). For small quark mass it is clear that an accurate determination of the slope  $A_p$  is necessary. But, as can be seen from Figs. 3(a) and 3(b), the slope is not the same for  $m_{\text{sea}} = m_{\text{valence}}$  and  $m_{\text{sea}} \ll m_{\text{valence}}$ , at least in the region of quark masses studied. In the latter case, at  $\beta=5.4$  there is a region for larger quark mass where the slope is much smaller (by about a factor of 2). One should also note the *substantial* deviations from linear (current-algebra) behavior for  $m_{\text{sea}} \ll m_{\text{valence}}$  and  $m_{\text{valence}}$  greater than about 60 MeV. This situation affects particularly the charmed-quark mass estimate, for which the larger slope estimate, corresponds to the assumption  $m_{\text{sea}} = m_{\text{valence}}$ , is inappropriate. Because both physical situations are considered here we were able to encompass a range of quark masses that ranges from the  $u$ ,  $d$ , to the  $c$  quark.

Figures 4(a) and 4(b) show the pseudoscalar-meson mass squared as a function of the quark mass, in physical units (GeV), both for the case  $m_{\text{sea}} = m_{\text{valence}}$  and for  $m_{\text{sea}} \ll m_{\text{valence}}$ , as well as in the case  $n_f = 0$  (no fermion loops) as obtained with Wilson fermions at  $\beta=6.0$  (Ref. 5). The present analysis substantially refines the one previously presented in Refs. 7 and 8, where the case  $m_{\text{sea}} \ll m_{\text{valence}}$  was only marginally discussed because of the lack of computed data. Also, in the following the results for  $n_f = 2$  ( $u, d$  quarks) will be estimated by interpolation between  $n_f = 0$  and  $n_f = 3$ .

Before quoting the values for the quark masses, some correction factors have to be taken into account. The previously published results were based mostly on the more plentiful data at  $\beta=5.4$ . The new data at  $\beta=5.3$  is completely consistent (within the errors) with the results at  $\beta=5.4$ . In fact the substantial overlap of the two data sets is a partial check on the overall procedure, the size of finite lattice corrections, the size of finite-volume corrections, and on the approximate scaling in the gauge coupling. A renormalization-group-invariant quark mass  $\tilde{m}_q$  can be obtained by including the appropriate anomalous dimension factor

$$\tilde{m}_q = m_q(a) \left[ \ln \frac{1}{a \Lambda_{\overline{\text{MS}}}} \right]^{4/9} \quad (35)$$

with  $\Lambda_{\overline{\text{MS}}} = 125(20)$  MeV for  $n_f = 3$  at the weaker coupling ( $\beta=5.4$ ) [which should be compared to  $\Lambda_{\overline{\text{MS}}} = 110(10)$  MeV for  $n_f = 0$  and  $\beta=6.0$ ]. In turn  $\tilde{m}_q$  can be related to the quark masses at any scale by the equation

$$m_q(\mu) = \tilde{m}_q \left[ \ln \frac{\mu}{\Lambda_{\overline{\text{MS}}}} \right]^{-4/9} \quad (36)$$

Including a further lattice correction [due to the different

renormalization properties of the fermions on a lattice and in the continuum,<sup>20</sup> which in the pure gauge case at  $\beta=6.0$  is estimated to give a reduction by  $Z_m^W \approx 0.70$  (Refs. 5 and 7)] one finds  $m(\mu=1 \text{ GeV}) \approx 1.14m(a)$ , or

$$\begin{aligned} m_u(1 \text{ GeV}) &\approx 1.4 \text{ MeV}, & m_d(1 \text{ GeV}) &\approx 2.5 \text{ MeV}, \\ m_s(1 \text{ GeV}) &\approx 50 \text{ MeV}, & m_c(1 \text{ GeV}) &\approx 970 \text{ MeV}, \end{aligned} \quad (37)$$

with a total error that is estimated at about 20%. We have used here the well-established result  $m_d/m_u = 1.8$  (Ref. 3). In the charmed-quark mass region it appears reasonable to assume that one has three *light* flavors. The charmed-quark mass quoted above is extracted from the experimental  $D$  and  $\eta_c$  charmed-meson masses. The two values deviate by less than 5% from each other and we use the average here. Note in particular that due to the lightness of the strange quark, one obtains a relatively large estimate for the invariant ratio  $m_c/m_s \approx 20$ . Furthermore it appears that for all three light quarks ( $u, d, s$ ) one has  $m_q \ll \Lambda_{\overline{\text{MS}}}$ , and this in turn would justify the use of  $n_f = 3$ . These values for the quark masses quoted above should be compared to the best estimates for  $n_f = 0$  (Refs. 5 and 7):

$$\begin{aligned} m_u(1 \text{ GeV}) &\approx 3.0 \text{ MeV}, \\ m_d(1 \text{ GeV}) &\approx 5.2 \text{ MeV}, \\ m_1(1 \text{ GeV}) &\approx 100 \text{ MeV}, \end{aligned} \quad (38)$$

with errors again around 20%. It is somewhat surprising that such a relatively strong flavor dependence goes into the estimates for the light-quark masses. Part of this effect is due to the quark loops causing substantial deviations from linearity in the (valence-) quark mass. We quote for comparison the (continuum QCD sum-rule) estimates of Gasser and Leutwyler<sup>3</sup>:

$$\begin{aligned} m_u(1 \text{ GeV}) &\approx 5.1 \text{ MeV}, & m_d(1 \text{ GeV}) &\approx 8.9 \text{ MeV}, \\ m_s(1 \text{ GeV}) &\approx 175 \text{ MeV}, & m_c(1 \text{ GeV}) &\approx 1350 \text{ MeV}. \end{aligned} \quad (39)$$

In conclusion, in the present lattice computations the quark masses turn out to be quite small, even allowing for substantial lattice errors and systematic effects due to the fermion algorithm.

## VII. CONCLUSIONS

The results presented here for light hadron spectroscopy at  $\beta=5.3$  and  $\beta=5.4$  appear to be in reasonable agreement with experiment and have not yet uncovered any substantial disagreement with the computations done without loops, partly due to the fact that the results presented here can still only be considered as qualitative. Future work will have to, among other things, reduce the systematic effects due to the fermion algorithm and refine the results presented in this paper. Surprisingly the light-quark masses have turned out to be quite small, and future calculations will have to check whether the results remain stable for even smaller quark masses and weaker coupling.

## ACKNOWLEDGMENTS

The calculations presented in this paper required a rather substantial amount of supercomputer time and were performed on the Cray X-MP 4/8 and the SCS-40 at the San Diego Supercomputer Center, which is operated by GA Technologies for the National Science Founda-

tion. The author would like to thank Dr. Sid Karin, director of the Center, for his continuous support of the project, and Dr. Wayne Pfeiffer for his generous help in the code optimization effort. This work was supported in part by the National Science Foundation under Grant No. NSF-PHY-8605552.

- <sup>1</sup>I. Bigi, Lectures at the 1987 Summer Institute of Particle Physics, SLAC Report No. SLAC-PUB-4521, January 1988 (unpublished).
- <sup>2</sup>Mark III Collaboration, I. E. Stockdale, SLAC Report No. SLAC-PUB-4466, 1987 (unpublished); J. Adler *et al.*, Phys. Rev. Lett. **60**, 1375 (1988).
- <sup>3</sup>J. Gasser and H. Leutwyler, Phys. Rep. **87**, 78 (1982).
- <sup>4</sup>H. Fritzsch, Nucl. Phys. **B155**, 189 (1979); H. Georgi and D. V. Nanopoulos, Phys. Lett. **82B**, 392 (1979); Nucl. Phys. **B155**, 52 (1979); T. Kitazoe and K. Tanaka, Phys. Rev. D **18**, 3476 (1978).
- <sup>5</sup>H. Hamber, Phys. Lett. B **178**, 277 (1986); see also L. Maiani and G. Martinelli, *ibid.* **178**, 261 (1986); S. Itoh, Y. Iwasaki, and T. Yoshie, *ibid.* **167**, 443 (1986).
- <sup>6</sup>G. Parisi, in *Architecture of Fundamental Interactions at Short Distances*, proceedings of Les Houches Summer School, Les Houches, France, 1985, edited by P. Ramond and R. Stora (Les Houches Summer School Proceedings, Vol. 44) (North-Holland, Amsterdam, 1987); I. Montvay, Rev. Mod. Phys. **59**, 263 (1987).
- <sup>7</sup>H. Hamber, Nucl. Phys. Proc. Suppl. **1A**, 133 (1987).
- <sup>8</sup>H. Hamber, Nucl. Phys. **B251** [FS13], 182 (1985); Phys. Lett. B **193**, 292 (1987).
- <sup>9</sup>F. Fucito, E. Marinari, G. Parisi, and C. Rebbi, Nucl. Phys. **B180** [FS2], 369 (1980); H. Hamber, E. Marinari, G. Parisi, and C. Rebbi, Phys. Lett. **124B**, 99 (1983); Nucl. Phys. **B225** [FS9], 475 (1983).
- <sup>10</sup>K. G. Wilson, Phys. Rev. D **10**, 2445 (1974).
- <sup>11</sup>M. Campostrini, K. Moriarty, J. Potvin, and C. Rebbi, Phys. Lett. B **193**, 78 (1987); M. Fukugita, S. Ohta, Y. Oyanagi, and A. Ukawa, *ibid.* **191**, 164 (1987); S. A. Gottlieb, W. Liu, D. Toussaint, R. Renken, and R. Sugar, Phys. Rev. Lett. **59**, 1513 (1987); M. P. Grady, D. K. Sinclair, and J. B. Kogut, Phys. Lett. B **200**, 149 (1988).
- <sup>12</sup>M. Fukugita, Y. Oyanagi, and A. Ukawa, Phys. Rev. Lett. **57**, 953 (1986); Phys. Rev. D **36**, 824 (1987); Phys. Lett. B **203**, 145 (1988).
- <sup>13</sup>H. Hamber, in *Proceedings of the Third International Conference on Supercomputing*, Boston, 1988, edited by L. Kartshev (ISI, Boston, MA, 1988); in *Proceedings of the Fermilab Conference on Lattice Field Theory* [Nucl. Phys. B Suppl. (in press)].
- <sup>14</sup>R. Woloshyn, T. Draper, K. Liu, and W. Wilcox, TRIUMF report, 1988 (unpublished); S. Gottlieb *et al.*, Nucl. Phys. **B263**, 704 (1986); H. Hamber, Phys. Rev. D **27**, 2239 (1983); T. A. DeGrand and R. Loft, Phys. Rev. D **38**, 954 (1988); C. Bernard *et al.*, *ibid.* **38**, 3540 (1988).
- <sup>15</sup>P. Langacker and H. Pagels, Phys. Rev. D **8**, 4595 (1973); **8**, 4620 (1973); **10**, 2904 (1974); H. Pagels, Phys. Rep. **16**, 219 (1975).
- <sup>16</sup>J. Gasser, Ann. Phys. (N.Y.) **136**, 62 (1981); J. Gasser and H. Leutwyler, Nucl. Phys. **B250**, 465 (1985); J. F. Donoghue, B. R. Holstein, and Y. C. R. Lin, Phys. Rev. Lett. **55**, 2766 (1985).
- <sup>17</sup>J. Donoghue and C. Nappi, Phys. Lett. **168B**, 105 (1986); see also S. Brodsky, J. Ellis, and M. Karliner, SLAC Report No. SLAC-PUB-4519, 1988 (unpublished); R. Jaffe and C. Korpa, Comments Nucl. Part. Sci. **17**, 163 (1987).
- <sup>18</sup>B. Meyer and C. Smith, Phys. Lett. **123B**, 62 (1983); G. Martinelli and Y. C. Zhang, *ibid.* **125B**, 77 (1983).
- <sup>19</sup>H. D. Politzer and M. B. Wise, Caltech Report No. CALT-68-1486, 1988 (unpublished).
- <sup>20</sup>A. Gonzales-Arroyo, G. Martinelli, and F. Yndurain, Phys. Lett. **117B**, 437 (1982); H. Hamber and C. M. Wu, *ibid.* **133B**, 357 (1983).